A Photoresponsive Receptor with a 10^5 Magnitude of Reversible Anion-Binding Switching

Jeffrey D. Einkauf,[a] Vyacheslav S. Bryantsev, [a] Bruce A. Moyer,*[a] and Radu Custelcean*[a]

[a]Dr. J. D. Einkauf, Dr. V. S. Bryantsev, Dr. B. A. Moyer, and Dr. R. Custelcean
Chemical Sciences Division
Oak Ridge National Laboratory
Oak Ridge, TN, 37831-6119, USA.
Email: moyerba@ornl.gov
custelceanr@ornl.gov

ABSTRACT

In a leap toward anion separation that uses only energy input for binding and release cycles, we report herein a new class of photoswitchable anion receptors featuring a diiminoguanidinium functionality that displays more than five orders of magnitude switched-off change in binding strength towards sulfate, a representative oxyanion, upon photoirradiation with UV light. *E*,*E*-2-pyridyl-diiminoguanidinium cation, synthesized as the triflate salt, binds sulfate with extraordinary strength in DMSO-d_6 owing to its bidentate guanidinium hydrogen bonding that can chelate the O–S–O edge of sulfate. The anion-binding site is essentially shut off upon photoisomerization to the *Z*,*Z* isomer, by intramolecular hydrogen bonds to the 2-pyridyl substituents, as supported by anion-binding titrations, theoretical calculations, and X-ray structural analysis. This approach will allow the development of advanced anion separation cycles that use only energy input and generate no chemical waste, and thus address challenging chemical separation problems in a more sustainable way.

Keywords

Anions; Guanidines; Photoswitches; Separations; Sulfate

INTRODUCTION

In combining selective binding with a chemical function, molecular recognition[1] has found many uses, from sensing a few molecules of analytes[2] to transport of ions across biological membranes[3] to separating radionuclides from millions of gallons of nuclear waste.[4] In the preponderance of these applications, the recognition agent or receptor must be cycled between bound and unbound states with a target guest species, whether the function is information storage, phase transformation, sensing, catalysis, or transport. The completeness of this cycling represents a measure of the overall efficiency of the selective function, affecting the resultant consumption of energy and chemicals and production of desired materials and unwanted wastes. Maximizing efficiency of cycling raises a dilemma: the stronger the binding, the more difficult the release.[5] Challenging separations problems involving very dilute species in complex media place a premium on strong binding, consequently requiring a means to drive the corresponding steep uphill release. Generally, the uphill reversal is accomplished with chemical swings such as pH, which though effective, require chemical inputs and produce waste. Thus, a pure energy input is a highly desirable green means of driving efficient binding and release cycles in selective separations. For example, photoirradiation could trigger the release of a guest species and its transfer into the aqueous phase in a liquid-liquid separation system. Alternatively, photoirradiation could trigger phase changes such as dissolution/crystallization that could be exploited for binding/release cycles.

Among the options for stimulated binding and release, photoswitching has emerged as an efficient approach to control ion binding by energy inputs. Shinkai pioneered photoresponsive cation binding as applied to separations in liquid-liquid systems using crown ethers containing azobenzene chromophores.[6] As coordination chemistry has expanded to include anion receptors,[7] photoswitched anion binding has naturally been explored more recently. A table of the available literature on photoswitched anion binding may be found in the Supporting Information (Table S1). Two of the strategies employed are illustrated in Fig. 1. Using azobenzene and stillbene photoresponsive chromophores reported so far for photoswitched anion receptors,[8-16] the more stable *E* isomer is converted to the *Z* isomer, which relaxes back to the *E* isomer either thermally or photochemically. Under irradiation, a photostationary state (PSS) is achieved with reported *E*:*Z* ratios generally indicating incomplete conversion. Among photoswitchable anion receptors, the maximum reported PSS *E*:*Z* ratio was 14:86 for a chiral 2,2'-dihydroxy-1,1'-dinaphthyl-appended stiff-stillbene in benzene.[8] Both *E* and *Z* forms may have measurable anion binding, and either form may possess the stronger binding, leading to switched-on or switched-off binding behavior depending on whether the anion-binding functionalities are rendered more or less effective in the produced *Z* isomer. The ratio of 1:1 binding constants is often taken as the measure of the magnitude of switched anion binding, an important indicator of maximum switching efficiency subject to the degree to which one isomer can be converted to the other and back again in a functioning cycle. As may be seen in Table S1, with a couple of exceptions, the change in anion binding constants so far reported is generally modest. Some of the more efficient photoswitchable anion receptors reported to date include a foldamer containing two azobenzene chromophores with an 84-fold reduction in Cl^- binding strength (Table S1, C), [9b] and a strapped calix[4]pyrrole receptor with an 8000-fold difference in chloride binding affinity between the *Z* and *E* isomers induced by the strain in its stiff-stilbene strap upon photoisomerization (Table S1, O).[9c] As shown for one example in Figure 1a, switched-on chelation has been the most common mechanism employed to effect the change in anion binding. In this case, both *E* and *Z* isomers possess exposed H-bond donor functionalities, such as urea groups, and the conversion to the *Z*

form effects the stronger binding via the chelate effect. Switched-off binding by internal blocking of binding site through hydrogen bonding was reported in only one example (Figure 1b), where the phosphoryl group in the *Z* configuration competes with the anion for H-bonding to the urea group.[16] The maximum weakening of binding was observed to be 2.5-fold in the case of dihydrogen phosphate anion. In all reported cases for photoswitched anion receptors, the responsive chromophore does not participate directly in the binding of the anion but rather controls the molecular configuration of the organic linker, and consequently the orientation and availability of the binding groups.

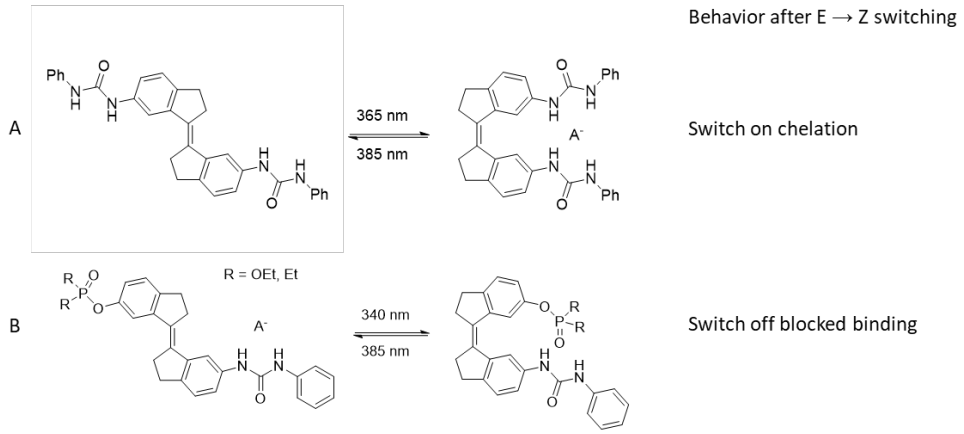

Figure 1. Photoswitching of anion binding of stiff-stillbene-based bis-urea receptors by Feringa and Wezenberg et. al., where the photoisomerization of the stiff-stillbene functionality produces: (A) switched-on chelation of an anion[14a] or (B) switched-off binding through blocking of the binding site.[16]

Current work in the field of photoswitchable anion receptors often takes inspiration from nature, taking advantage of the hydrophobic effect, sequestering hydrophobic molecules inside binding pockets.[10] Initial studies employed an indocarbazole-based foldamer that can adopt helical conformations providing a tubular cavity for anion binding in water; however, no photocontrol was attempted.[11] Flood and coworkers have taken this concept further by using UV light to sequester a wide range of anions, controlling the size of the helical quaternary structure and function via anion binding through azo –N=N– bonds installed on the foldamer.[9a,b] Other groups have been able to photoisomerize stiff-stilbene oligomer scaffolds decorated with urea anion-binding motifs to form weakly binding *E* forms and strongly binding Z forms with dihydrogenphosphate using near-UV light, with moderate photoconversion ratios.[12] Aside from bioinspired receptors, an acylhydrazone-based photoswitch with two separate binding sites for cations and anions has been reported; along with a multistep synthesis, cations Li^+, Na^+, K^+, and Bu_4N^+ and anions Ph_4B^-, Cl^-, Br^-, and I^- were studied, revealing limited selectivity between cation and anion combinations.[13] Notable photoswitchable systems by Feringa and coworkers incorporate the photoactive stiff-stillbene group to effect a conformational switch with light, while urea groups participate in binding.[12, 14] This general framework and its analogs have been used to study a wide range of anions including Cl^-, Br^-, NO_3^-, $CH_3CO_2^-$, $H_2PO_4^-$, and HSO_4^- with maximum binding constants of 7.5×10^3 M^{-1} for $H_2PO_4^-$ in DMSO. Another approach to anion recognition by Flood and coworkers[9a,b, 10, 15] utilizes a photofoldamer between helix and random coil states to alter the affinity switching of chloride guests, which has since been expanded to binding of 11 different anions (Cl^-, Br^-, NO_2^-, I^-, NO_3^-, SCN^-, BF_4^-, ClO_4^-, ReO_4^-, PF_6^-, SbF_6^-) and the binding behavior changes from single to double helixes with increasing anion size. Binding

constants for the 1:1 complexes were as high as 2.0×10^4 M^{-1} for I^- in MeCN. In both examples, the PSS achieved is not quantitative, with typical values of 42:58 (*E:Z*) for stiff-stillbene systems and 16:29:55 (*trans-trans:cis-trans:cis-cis*) for foldamers.

In view of the precedents already established with the photoisomerization of imine and hydrazone groups,[17] we hypothesized that the imine bond in iminoguanidinium groups would be responsive to *E*–*Z* photoisomerization, resulting in switching between anion binding and release. Guanidinium groups in general have proven effective for oxyanion binding owing to the complementarity of their dual N–H hydrogen-bond donors to oxyanion O–X–O edges.[18],51 Related iminoguanidinium derivatives[19] in particular provide both synthetic versatility and the potential for switched binding. As shown in Figure 2, the pair of N–H groups available for directed oxyanion binding in the *E,E* isomer could in principle be deactivated by appending 2-pyridyl groups that can act to close off the binding site by intramolecular hydrogen bonding in the *Z*,*Z* photoisomer. Following this logic, photoswitching between the open *E*,*E* and closed *Z*,*Z* photoisomers will thus provide a binding–release mechanism for efficient oxyanion separations. Herein, we introduce the first example of photoisomerization using an iminoguanidinium cation, as specifically demonstrated using 2-pyridyl-diiminoguanidinium (2PyDIG) and corresponding photoswitched binding of the model oxyanion sulfate. This receptor is easily prepared in one step by condensation of 2-pyridinecarboxaldehyde with *N*,*N*'-diaminoguanidine hydrochloride.[20] Photoisomerization in DMSO-d_6 with UV light was monitored through ^{1}H NMR and UV-vis spectroscopies, supported by density functional theory (DFT) electronic-structure calculations and X-ray crystal structures of both the sulfate-bound *E,E* form and the nonbinding *Z,Z* photoisomer. Upon photoconversion, the binding of sulfate is essentially shut off in the *Z,Z* form, resulting in a five-orders-of-magnitude light-induced reversible switching of anion-binding strength, as determined by UV-absorption and ^{1}H NMR titrations, which to the best of our knowledge is the largest photoinduced change in anion-binding strength yet reported.

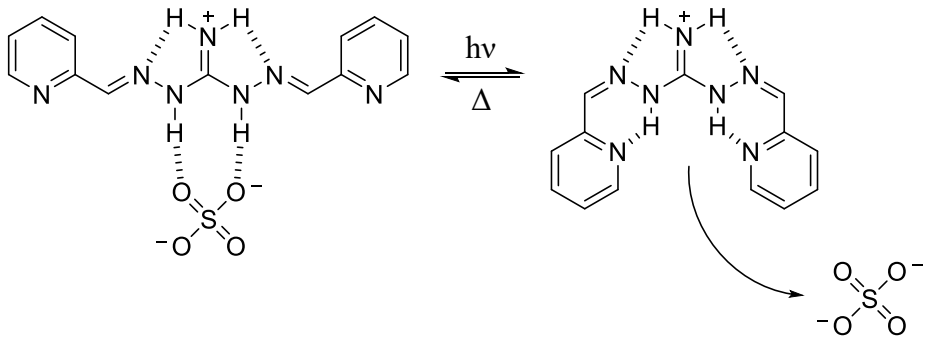

Figure 2. Structural changes and binding behavior anticipated in the proposed photoswitching of the 2PyDIG cation and the corresponding sulfate anion binding upon irradiation with UV light and thermal relaxation. Hydrogen bonds are marked as dashed lines.

RESULTS AND DISCUSSION

Photoisomerization and Thermal Relaxation Behavior

^{1}H NMR spectroscopy confirmed the photoconversion of the open *E*,*E* to the closed *Z*,*Z* form of 2PyDIG. The 2PyDIG receptor was initially prepared as the chloride salt, followed by an exchange to the triflate (TfO^-) salt, where triflate was expected to be much less competitive in anion-binding

studies. To probe the ability of 2PyDIG to photoisomerize in the presence of UV light, its triflate salt in DMSO-d_6 (*ca.* 1 mM and 10 mM concentrations) was photoirradiated with an unfiltered Hg vapor lamp for 6 h (see Supporting Information for details). The ^{1}H NMR spectrum of the open *E*,*E*-2PyDIG·HOTf (Figure 3) at 1 mM in DMSO-d_6 consists of only seven peaks, consistent with its symmetry: four peaks at δ = 8.67, 8.39 ppm as doublets and 7.98 and 7.54 ppm as triplets corresponding to pyridine protons, a broad singlet at 8.74 ppm corresponding to the guanidinium protons (=NH_2), a slightly broad overlapping singlet at 8.42 ppm from the imine proton (–N=CH), and lastly, the most downfield resonance at 12.21 ppm (not shown in Figure 3) is assigned to the guanidinium –N–H protons. After UV irradiation (Hg vapor lamp), the photoconverted *Z*,*Z* photoisomer also gives rise to seven unique resonances different from those of the *E*,*E* form, initially with no observable *E*,*E* isomer present above experimental noise in the case of the 1 mM solution. Resonances corresponding to pyridine proton signals at 8.18 and 7.68 ppm appear as triplets, while a set of doublets, one at 8.80 ppm and the second at 7.91 ppm overlap with the sharp singlet corresponding to the imine proton at 7.96 ppm. The guanidine N–H proton resonance shifts downfield from 12.21 in the *E*,*E* isomer to 15.05 ppm (Supporting Information, Figure S2) after photoirradiation to the *Z*,*Z* form. This significant downfield shift is indicative of a drastic change in environment around the proton, consistent with the presence of intramolecular hydrogen bonding. The chemical shifts of the non-exchangeable protons of two forms align closely with DFT-generated ^{1}H NMR spectra,[21] except for the imine protons, which are systematically shifted to higher field (Supporting Information , Figure S4).[22] While different populations of rotational isomers are expected based on DFT calculations (Supporting Information, Figure S12), the simplicity of the NMR spectra suggests a fast exchange about the C–N bonds at room temperature

for both the E,E and Z,Z forms. Lastly, no evidence of the intermediate *E*,*Z* isomer could be detected in the NMR spectra, pointing to its transient nature under these conditions.

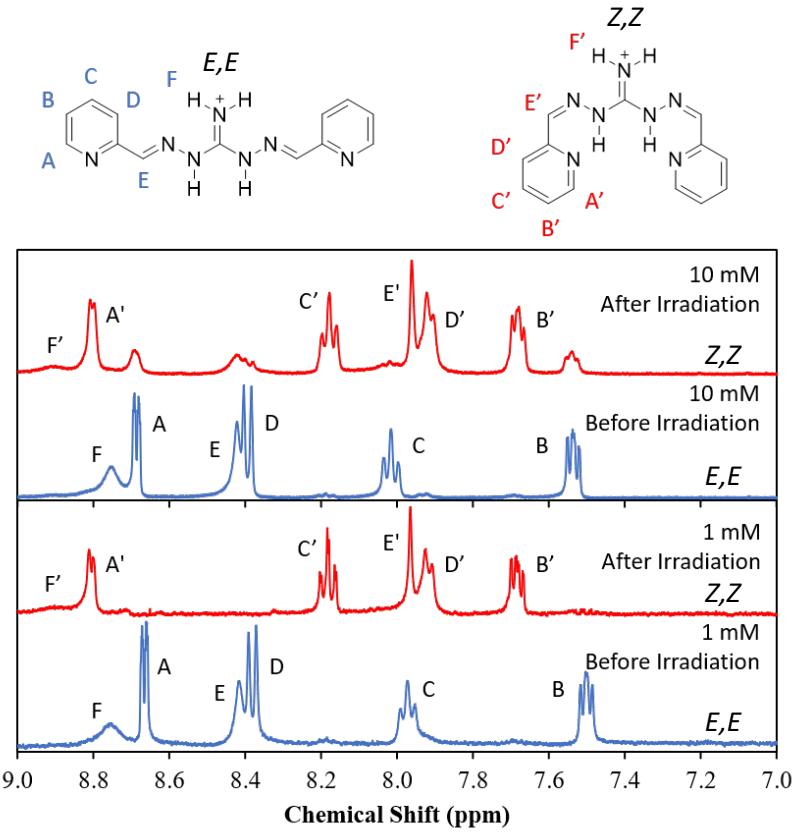

Figure 3. ^{1}H NMR (400 MHz) spectra of the aromatic region for 1.01 mM (bottom) and 10.03 mM (top) 2PyDIG·HOTf in DMSO-d_6 at 24 °C before (blue) and after (red) 1 h UV photoirradiation.

Stirred solutions of 1.5 and 10 mM 2PyDIG exposed to UV light reach photostationary states (Figure ***4*** 4), as indicated by the evolution of their ^{1}H NMR spectra monitored at various time intervals (Supporting Information, Figure S2). Thus, irradiation of freshly prepared samples causes a progressive disappearance of the *E*,*E* isomer signals, while a new set of signals from the *Z*,*Z* isomer grows in. At 1.5 mM, the *E*,*E* isomer (with initially 5.5 ± 0.5% *Z*,*Z* isomer), reaches 95.6 ± 0.4% photoconversion to the *Z*,*Z* isomer in less than 15 min; at the 95% confidence level, this is indistinguishable from complete conversion. Visual inspection of the chemical-shift region 8.35–8.70 ppm shows no apparent trace of the *E*,*E* isomer remaining. In the 10 mM solution, however, it takes a little more than 2 h to reach a PSS consisting of 67.7 ± 4.4% *Z*,*Z* isomer. Thus,

while under conditions of low concentration the degree of conversion at PSS is exceptional for a photoswitched anion receptor, more typical behavior is obtained at higher concentrations.

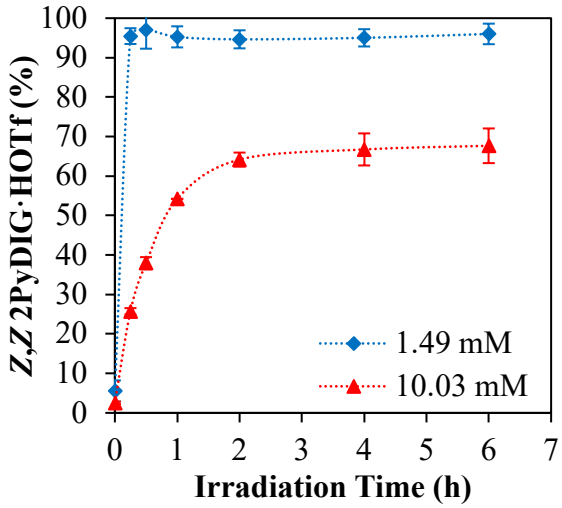

Figure 4. Conversion of 1.49 mM (blue) and 10.03 mM (red) *E*,*E* 2PyDIG·HOTf to the *Z*,*Z* photoisomer over the course of 6 h at 24 °C under UV irradiation in DMSO-d_6. Dotted lines are for visual aid.

The absorption maximum of the 2PyDIG cation in its near-UV spectrum undergoes a slight bathochromic shift from 315 nm to 320 nm during UV irradiation as a result of *E*,*E* to *Z*,*Z* conversion, as depicted in Figure 5. The absorption spectrum of 2PyDIG·HOTf in DMSO-d_6 contains features between 260–350 nm, which are attributed mainly to allowed π–π* transitions that dominate much weaker n-π* transitions involving pyridine lone pairs, while the transition involving the lone pairs of the C=N groups occur at higher energies.[23] Shoulders below 285 nm as well as the main absorption bands in the range 310–350 nm correspond to the π–π* transitions of the extended conjugated systems involving both the iminoguanidinium moiety and the pyridyl rings. The transition at 440 nm is tentatively assigned to aggregates of the 2PyDIG receptors in solution, as this peak disappears upon dilution. The minor bathochromic shift upon photoisomerization from the *E*,*E* to *Z*,*Z* is expected, and has been previously reported in acylhydrazone systems, as both isomers retain their planarity.[17c]

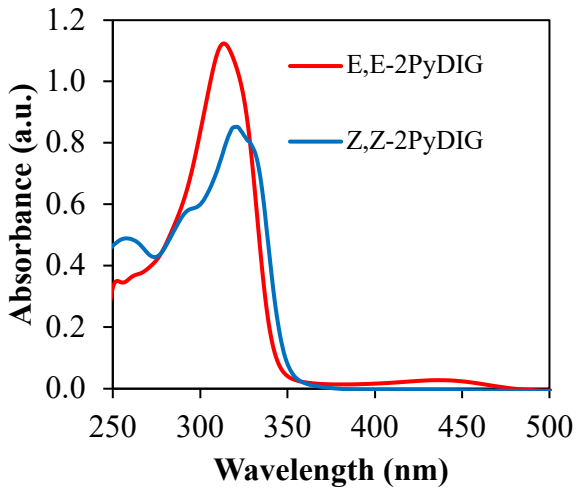

Figure 5. Absorption spectrum of 1.21 mM *E*,*E*- (λ_{max} = 315 nm) and *Z*,*Z*-2PyDIG·HOTf (λ_{max} = 320 nm) in DMSO-d_6.

Both photoirradiated and freshly prepared (nonirradiated) 2PyDIG·HOTf solutions behave as T-type photoswitches,[24] thermally relaxing to a common thermal equilibrium of 70.5 ± 0.9% *E*,*E* isomer. Thermal relaxation was investigated by monitoring the photoirradiated solutions at 24 °C and 50 °C (Figure 6). At 10 mM, thermal equilibrium is reached after 4 days at 24 °C, and less than 24 h at 50 °C. Unirradiated *E*,*E* isomer thermally equilibrates to the same state in 14 d at 24 °C. These results indicate two underlying processes that lead to a common equilibrium point: the spontaneous conversion from EE to ZZ under normal visible light, and the back reaction from ZZ to EE under normal visible light and thermal heating. The thermal relaxation equilibrium back to *E*,*E* from *Z*,*Z* corresponding to Eq. 1 has an implied equilibrium constant of 2.38(8) that is independent of temperature, suggesting an enthalpy and entropy change close to zero.

$$(E,E)^+ \underset{K_{relax} = 2.4}{\overset{h\nu}{\rightleftharpoons}} (Z,Z)^+ \qquad (1)$$

An intramolecular imine-enamine tautomerization that lowers the energy barrier between *Z* to *E* isomers through an inversion mechanism has been hypothesized.[25] In our system, the reversion from the *Z*,*Z* to *E*,*E* isomer at 24 °C appears to follow a second-order process (Supporting Information, Figure S5), implying a bimolecular isomerization mechanism possibly facilitated by intermolecular proton transfer. The concentration-dependence of the reversion rate may explain in part the decrease in the degree of conversion to the *Z*,*Z* isomer at PSS at 10 mM 2PyDIG shown in Figure 4. Efforts to understand both the forward and reverse processes in more detail are currently underway. Interestingly, the thermal relaxation behavior (both rate and end state) does not change upon the addition of 10 or 50 mM excess triflate (Supporting Information, Figure S6), indicating this anion acts as a spectator and does not facilitate the reversion. We show, however, that the presence of sulfate drives the reversion to near completion (vide infra). Finally, photoirradiation and thermal relaxation of a 10 mM 2PyDIG solution can be cycled several times in DMSO without signs of fatigue (Supporting Information, Figure S7). Cycles consisted of 6-hour irradiation times followed by 24-hour dark equilibrations, the percent *Z*,*Z* isomer switching between values of 69% and 25%, respectively. Cycling experiments at lower concentrations were

not practical since the time required for a 1 mM 2PyDIG solution to reach thermal equilibrium, even at elevated temperatures, is greater than 20 days.

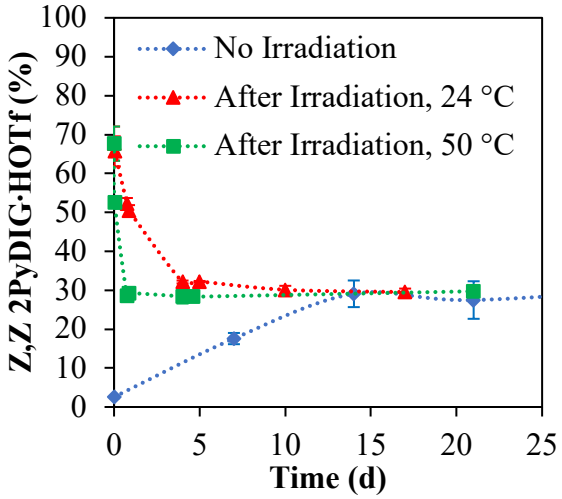

Figure 6. Thermal relaxation of 10.03 mM 2PyDIG·HOTf in DMSO-d_6 after irradiation, at 24 (red) and 50 °C (green), and the non-irradiated *E*,*E* isomer at 24 °C (blue) converging at a thermal equilibrium. Dotted lines are for visual aid.

X-ray Crystal Structure Analyses of E,E and Z,Z 2PyDIG Photoisomers

The crystal structure of the open *E*,*E*-2PyDIG receptor, as sulfate salt, highlights the characteristic bidentate N–H hydrogen-bonding from two guanidinium cations along opposite O–S–O edges of sulfate.[26] As depicted in Figure 7, the 2PyDIG cation is planar, with a dihedral angle of 177.7° between carbon atoms of the two pyridine rings. A 2:1 guanidinium:sulfate binding is found in the crystal, with the two 2PyDIG cations nearly orthogonal to each other (104.5°), and with measured N–H···O contact distances varying between 1.82 and 1.84 Å. The crystal packing involves mainly N–H···O hydrogen bonds between the $–NH_2$ guanidium protons and solvent molecules, combined with stabilizing π-π interactions (Supporting Information, Figure S10), with distances between pyridine rings of 4.38 Å and a slippage angle of 49.14°.[27] A similar structural motif has been reported for sulfate binding by *N*,*N*-bis(2-pyridyl)guanidinium, sharing the dual hydrogen bonding to opposite O–S–O edges and stabilizing intramolecular hydrogen bonding of the guanidine $–NH_2$ group to the pyridines.[26]

As hypothesized, the structure of the photoisomerized 2PyDIG reveals the *Z*,*Z* configuration and stabilizing intramolecular hydrogen bonds to the pyridine N atoms (Figure 8). Although the unsymmetrical conformer shown was observed in the crystal instead of the symmetrical one depicted in Figure 2, the guanidine hydrogen atoms engaged in hydrogen bonds with pyridine N atoms are presumably inaccessible for anion binding. Accordingly, attempts to crystallize the *Z*,*Z* photoisomer with various oxyanions (SO_4^{2-}, NO_3^-, ReO_4^-, ClO_4^-, and *p*-toluenesulfonate) were not successful. However, *Z*,*Z*-2PyDIG could be crystallized from methanol using a large, non-coordinating anion, tetraphenylborate, before the cation underwent thermal relaxation. The rotation about one central guanidine C–N bond was not entirely expected because of the presumed loss of one intramolecular hydrogen bond from the $–NH_2$ group to the imine N atom, but DFT analysis shows a negligible energy difference between the two geometric isomers

(Supporting Information, Figure S12). The isomer maintains planarity upon conversion, while the stabilizing intramolecular hydrogen bonds between the N–H guanidinium protons and pyridine N atoms have measured contact distances of 1.971 and 1.969 Å. Hydrogen bonding between guanidinium $–NH_2$ protons and solvent molecules is also present in the crystal packing, and so is the π-stacking between 2PyDIG pyridine rings,[27] with distance between centroids of 3.60 Å and a slippage angle of 21.9°.

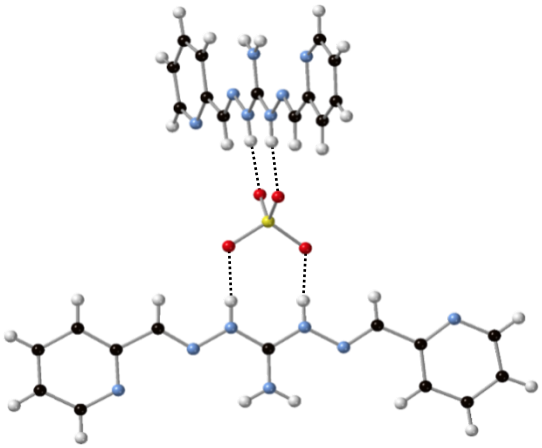

Figure 7. Crystal structure of *E*,*E*-2PyDIG$_2$·H_2SO_4 highlighting the 2:1 sulfate binding by the 2PyDIG cations. Yellow spheres are sulfur atoms, red spheres are oxygen atoms, blue spheres are nitrogen atoms, black spheres are carbon atoms, and white spheres are hydrogen atoms. Solvent molecules have been removed for clarity. Hydrogen bonds to sulfate are depicted as dotted lines.

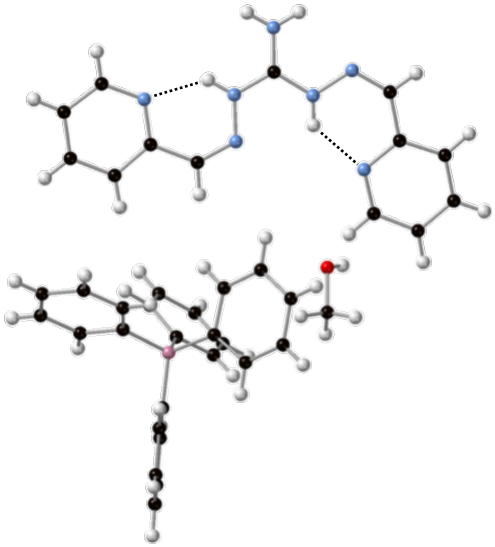

Figure 8. Crystal structure of the *Z*,*Z*-2PyDIG·$HBPh_4$ photoisomer. Red spheres are oxygen atoms, blue spheres are nitrogen atoms, black spheres are carbon atoms, magenta spheres are boron atoms, and white spheres are hydrogen atoms. Disordered solvent molecules have been removed for clarity. Intramolecular NH···N hydrogen bonds are depicted as dotted lines.

Sulfate Binding by the E,E-2PyDIG Cation

UV-vis absorption spectroscopy reveals the *E*,*E*-2PyDIG cation binds sulfate very strongly in DMSO-d_6. Titration of a 1 mM solution of *E*,*E*-2PyDIG·HOTf with tetramethylammonium sulfate results in a change in the intensity at the absorption maximum (Figure 9). The absorbance maximum at 315 nm increases approximately 25% in the range 0 to 0.5 mole ratio sulfate:2PyDIG, followed by a 65% decrease in absorbance from 0.5 to 3.0 mole ratio. The change in absorbance is attributed to sulfate binding via hydrogen bonding, as found in the crystal structure, ruling out proton transfer observed elsewhere in the presence of basic anions such as fluoride.[28] If this were the case, a transition at 376 nm would arise from the neutral 2PyDIG receptor (Supporting Information, Figure S36). The titration was repeated and analyzed three times (SI, Figures S14-S16), with the profiles of absorbance values as a function of sulfate-to-receptor mole ratio showing the same features in all three trials. A three-species complexation model is required to fit the data, assuming free *E*,*E*-2PyDIG cation and sulfate anion as reactant species. In the titration of sulfate into the receptor solution, the first complex that appears has the same stoichiometry as found in the crystal structure (Figure 7), $[(2PyDIG)_2(SO_4)]$, indicating this 2:1 complex is highly stable. Above a sulfate-to-receptor mole ratio of 0.5, further addition of sulfate generates the 1:1 complex $[(2PyDIG)(SO_4)]$, which apparently adds an additional sulfate to give the $[(2PyDIG)(SO_4)_2]$ complex past a sulfate-to-receptor mole ratio of 1.0. Table 1 summarizes the averaged binding constants and the corresponding formation equilibria (Eqs. 2–4).

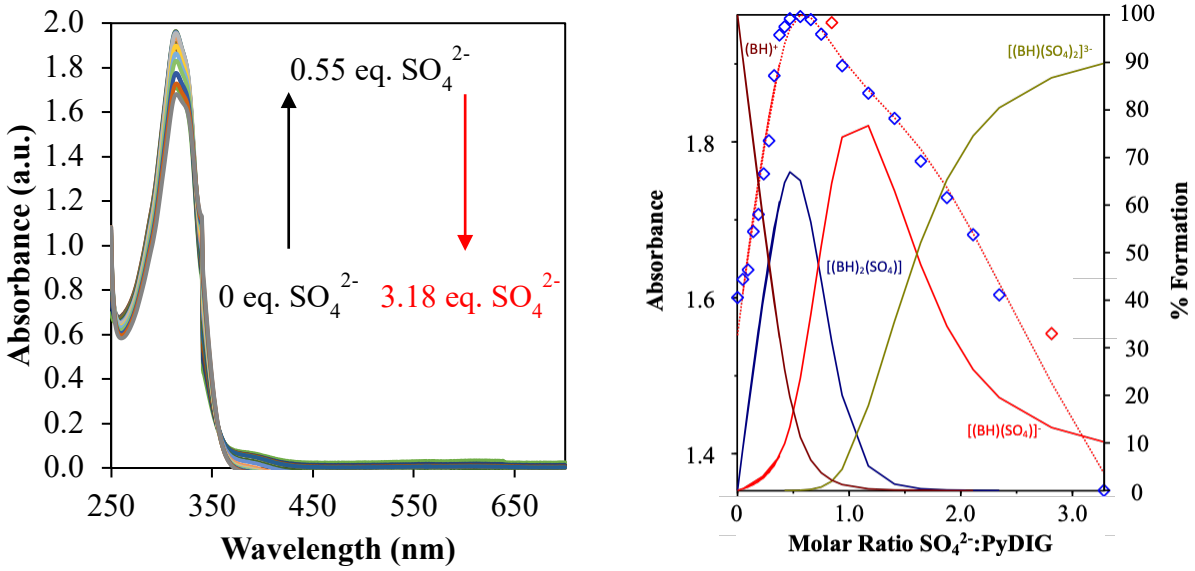

Figure 9. Absorbance (left) and speciation plot (right) of the UV-Vis titration of *E*,*E*-2PyDIG·HOTf with tetramethylammonium sulfate relative to 2PyDIG·HOTf in DMSO-d_6 at 24 °C. Here, BH represents the monoprotonated cationic form of 2PyDIG.

Parallel ^{1}H NMR titrations in DMSO-d_6 produce statistically identical results as found by UV-vis titrations (Table 1). Titration of a 1 mM solution of *E*,*E*-2PyDIG·HOTf with tetramethylammonium sulfate results in small but consistently measurable downfield shifts ($\Delta\delta$ = 0.04 ppm, (Figures S21, S24, S27, S30) of the guanidinium N–H protons. The observed change in

chemical shift, while minor, is not uncommon in hydrogen-bonding anion-binding systems.[8, 29] While the small change in chemical shift may seem at odds with the large binding constants determined, we suspect that, as found previously with sulfate binding by guanidinium receptors in competitive hydrogen-bonding solvents, the anion binding may be entropy-driven due to significant solvent interactions and reorganizations.[30] Although the iminoguanidinium group is weakly acidic, with typical pK_a values in the range of 7–9,[31] the ^{1}H NMR spectrum of the neutral *E*,*E*-2PyDIG isomer (Supporting Information, Figure S36) does not match the spectrum obtained in the titration of *E*,*E*-2PyDIG cation with sulfate, thus ruling out deprotonation during titration. The titration was repeated and analyzed four times (Figures S21-S34). Again, a three-species complexation model had to be employed to fit the data. The speciation profiles of chemical shifts as a function of sulfate-to-receptor mole ratio show the same features in the four trials and follow a similar trend observed in the UV-vis titrations. Upon addition of sulfate into the 2PyDIG solution, the first complex that appears again is the [(2PyDIG)$_2$(SO$_4$)] at a sulfate-to-receptor mole ratio of 0.5, also reported with absorption-based titrations. Further addition of sulfate generates the 1:1 complex [(2PyDIG)(SO$_4$)], at 1.0 sulfate to receptor ratio. An additional sulfate gives the [(2PyDIG)(SO$_4$)$_2$] complex beyond a sulfate-to-receptor mole ratio of 1.0.

Table 1. Comparison of fitted sulfate-binding constants corresponding to formation equilibria 2–4 obtained from the ^{1}H NMR and UV-vis titrations.[a]

			E,*E*	*E*,*E*
Equilibrium	Eq.	Constant	NMR Value[b]	UV Value[c]
(*E,E*-2PyDIG)$^+$ + SO$_4^{2-}$ $\rightleftharpoons$ [(*E,E*-2PyDIG)(SO$_4$)]$^-$	(2)	log β_{11}	7.40 ± 0.92	7.21 ± 0.48
2(*E,E*-2PyDIG)$^+$ + SO$_4^{2-}$ $\rightleftharpoons$ [(*E,E*-2PyDIG)$_2$(SO$_4$)]	(3)	log β_{21}	11.67 ± 0.95	11.25 ± 0.68
(*E,E*-2PyDIG)$^+$ + 2SO$_4^{2-}$ $\rightleftharpoons$ [(*E,E*-2PyDIG)(SO$_4$)$_2$]$^{3-}$	(4)	log β_{12}	12.23 ± 1.18	11.70 ± 0.95

[a]In each titration, tetramethylammonium sulfate was added to *ca.* 1 mM 2PyDIG·HOTf in DMSO-d_6 at 24 °C. [b]Average of four titration measurements. [c]Average of three titration measurements. Uncertainty for each value as shown represents the precision of the four trials; the standard error of the mean can be obtained by dividing by the square root of the number of replicates. Constants shown are concentration quotients.

In comparison to published binding constants, *E*,*E*-2PyDIG cation binds sulfate with comparable if not superior strength. Values for the binding constants as an average of the UV-vis and NMR experiments are shown in Table 2. The 1:1 and 2:1 binding constants of 7.25 ± 0.43 (log β_{11}) and 11.39 ± 0.55 (log β_{21}) shown in Table 2 are the highest recorded for any monofunctional guanidinium receptor in a polar medium (see Supporting Information for comparable systems).[30, 32] The highest comparable sulfate binding was reported by Kobiro and Inoue,[32a] for a receptor containing 4-(*N*,*N*-dimethylamino)benzoate group tethered to a bicyclic guanidinium subunit. This receptor forms 1:1 and 2:1 adducts with sulfate with stepwise binding constants of 1.53×10^6 M^{-1} and 4.84×10^4 M^{-1} in CD$_3$CN, respectively, corresponding to log β_{11} and log β_{21} values of 6.18 and 10.86. Although these values are approximately an order of magnitude lower than those shown in Table 2 for *E*,*E*-2PyDIG, within the precision of our measurements, the values are statistically comparable. However, DMSO possesses strong electron-pair donor strength compared with CH$_3$CN and therefore would solvate *E*,*E*-2PyDIG more strongly by accepting hydrogen bonds, thereby competing with anion binding. Due to this solvation-based competition effect, the superior sulfate binding strength of *E*,*E*-2PyDIG is likely to be real. The strength of the *E*,*E*-2PyDIG cation in binding sulfate may be attributed to the greater acidity of the iminoguanidininum group. While guanidinium cations are very weakly acidic in water (p*K*a = 13.6),[33] iminoguanidinium cations are several orders of magnitude more acidic, sufficient to dissociate under near-neutral conditions

(pK_a values of 7–9)[31]. Thus, in the absence of proton transfer (ruled out here, *vide supra*), the hydrogen-bond-donor strength of the receptor is maximized.

With larger amounts of sulfate added to *E*,*E*-2PyDIG, the fitting indicates the formation of a 1:2 adduct with a log β_{12} of 11.91 ± 0.74 M^{-1} (Table 2) This putative addition of the second sulfate to the 1:1 adduct is surprisingly strong (log K_{12} = 4.7 ± 1.5), given the negative charge of the 1:1 complex and competition for hydrogen bonding by the first sulfate. We suspect that the tetramethylammonium cations present may be moderating the coulombic repulsion. At *E*,*E*-2PyDIG concentrations greater than 1 mM in DMSO, a precipitation reaction begins at a sulfate:*E*,*E*-2PyDIG mole ratio of 2, which prevents carrying out titrations at higher concentrations of *E*,*E*-2PyDIG.

Sulfate Binding by the Z,Z-2PyDIG Cation

Photoisomerization to the *Z*,*Z*-2PyDIG isomer results in a marked decrease in sulfate binding. Under the same conditions used for the titrations of the *E*,*E* isomer, the ^{1}H NMR spectra of 1.1 mM *Z*,*Z*-2PyDIG in DMSO-d_6 (after 2 h irradiation of the *E*,*E* isomer) show no measurable changes in chemical shifts upon addition of tetramethyl ammonium sulfate. However, a significant interaction can be quantified in the UV-vis spectra in DMSO-d_6 through the *Z*,*Z* isomer's absorption maximum at 320 nm, which increases in intensity with the addition of sulfate (Figure 10). The same speciation model used for the *E*,*E* titrations was again needed to adequately fit the data. Binding constants averaged over three titrations are given in Table 2. Slight deviations from the model are observed at low sulfate-to-receptor mole ratio (<0.03), consistent with the minor amount of unconverted *E*,*E*-2PyDIG remaining in solution, which out-competes the *Z*,*Z* form for sulfate binding until the minor amount of *E*,*E* isomer is consumed. Effectively, if a small amount of *E,E* isomer remains in the Z,Z solutions after photoirradiation, that amount being on the order of 0.03 mM in our experiments, represents the lower limit of sulfate that can be regulated by photoirradiation.

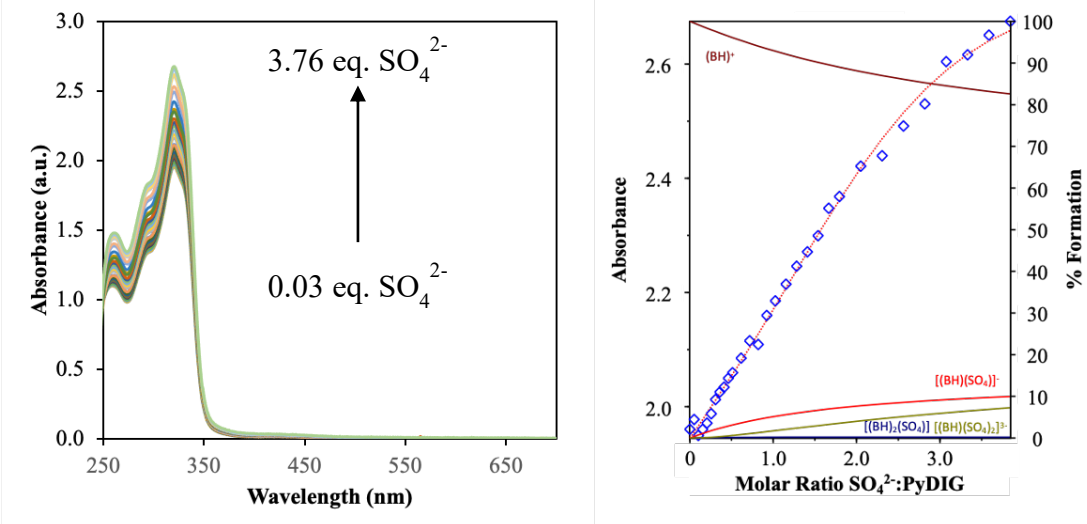

Figure 10. Absorbance (left) and speciation plot (right) of the UV-Vis titration of *E*,*E*-2PyDIG·HOTf with tetramethylammonium sulfate relative to 2PyDIG·HOTf in DMSO-d_6 at 24 °C. Here, BH represents the monoprotonated cationic form of 2PyDIG.

Table 2. Comparison of sulfate binding constants for *E*,*E* and *Z*,*Z* isomers of 2PyDIG.

			E,*E*[a]	*Z*,*Z*[b]	*E*,*E*–*Z*,*Z*
Equilibrium	Eq.	Constant	Avg Value[b]	UV Value[c]	Difference
$(2PyDIG)^+ + SO_4^{2-} \rightleftharpoons [(2PyDIG)(SO_4)]^-$	(2)	$\log \beta_{11}$	7.25 ± 0.43	1.85 ± 0.15	5.40 ± 0.45
$2(2PyDIG)^+ + SO_4^{2-} \rightleftharpoons [(2PyDIG)_2(SO_4)]$	(3)	$\log \beta_{21}$	11.39 ± 0.55	3.08 ± 0.09	8.31 ± 0.56
$(2PyDIG)^+ + 2SO_4^{2-} \rightleftharpoons [(2PyDIG)(SO_4)_2]^{3-}$	(4)	$\log \beta_{12}$	11.91 ± 0.74	4.00 ± 0.19	7.91 ± 0.76

[a]Precision-weighted average of the values shown in Table 1 for the constants shown for UV-vis and NMR titrations. [b]Average of three titrations (see Supporting Information) in which tetramethylammonium sulfate was added to *ca.* 1 mM *Z*,*Z*-2PyDIG·HOTf in DMSO-d_6 at 24 °C following 2 h irradiation of the initial *E*,*E* isomer. Uncertainty for each value as shown represents the precision of the three trials; the standard error of the mean can be obtained by dividing by the square root of the number of replicates. Constants shown are concentration quotients.

2PyDIG Photoswitching in the Presence of Sulfate

Photoisomerization of *E*,*E*-2PyDIG in the presence of sulfate does not affect the efficiency of photoisomerization to the *Z*,*Z* isomer; however, a near quantitative thermal relaxation to the *E*,*E* isomer is observed. A solution of *ca.* 10 mM 2PyDIG·HOTf in DMSO-d_6 was monitored by ^{1}H NMR spectroscopy (Supporting Information, Figure S37–S39). After addition of 0.5 mol ratio of sulfate to *E*,*E*-2PyDIG before irradiation, the relative *E*,*E* to *Z*,*Z* ratios remain unchanged according to ^{1}H NMR (93.1 ± 1.2% and 92.8 ± 1.4% *E*,*E*, before and after sulfate addition, respectively), accompanied with a slight downfield shift of the NH guanidine protons ($\Delta\delta$ = 0.02 ppm). After 2 h of UV irradiation, the remaining 32.5 ± 3.8% *E*,*E* isomer at PSS as compared with 32.3.± 4.4% *E*,*E* isomer at PSS in the absence of sulfate suggests that the sulfate anion does not play a controlling role in the photoisomerization process. Thermal relaxation from PSS was monitored at 50 °C in the presence of sulfate, with thermal equilibrium returning to 91.2 ± 1.4% *E*,*E* isomer after 36 h with no further change at 60 h, almost to the pre-irradiation state. This process was repeated upon addition of 0.5 and 1.0 mol ratio sulfate post-irradiation, with similar PSS and thermal equilibrium states being achieved compared with sulfate addition pre-irradiation (Table 3). The expected near-complete reversion to the *E*,*E* isomer reflects the driving force of sulfate binding by the *E*,*E* isomer (Eq. 5). In a catch-and-release cycle, the more complete reversion to the *E*,*E* isomer in the dark effectively represents an increase in capacity.

Table 3. Relative degree of isomerization of *E*,*E*-$2PyDIG^+$ in the absence or presence of sulfate during photoisomerization and thermal relaxation.

	Relative Amount of *E*,*E*-$2PyDIG^+$ (%)			
	Control; no SO_4^{2-} added	SO_4^{2-} added before irradiation	SO_4^{2-} added after irradiation	SO_4^{2-} added after irradiation
Mol ratio SO_4^{2-} :$2PyDIG^+$	0	0.5	0.5	1.0
Before irradiation	97.4 ± 0.6	91.1 ± 1.2%	95.1 ± 1.4	93.4 ± 2.9
After irradiation	32.3 ± 4.4	32.5 ± 3.8	33.2 ± 5.3	31.0 ± 4.7
Thermal equilibrium	70.5 ± 0.9	91.2 ± 1.4	93.1 ± 3.3	91.6 ± 1.9

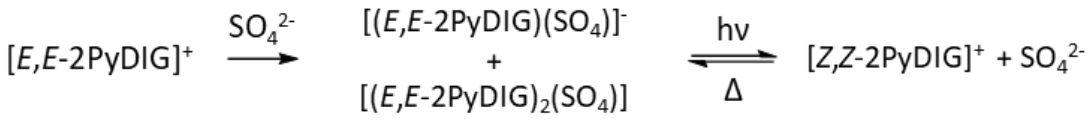

(5)

Photoswitching of Sulfate Binding

Dramatic switched-off sulfate binding occurs upon photoisomerization of *E*,*E*-2PyDIG into the *Z,Z* isomer, as determined by ^{1}H NMR and UV-vis absorption spectroscopies in DMSO-d_6. As shown in the difference column of Table 2, the initially strong binding strength of 2PyDIG upon photoirradiation of its *E*,*E* isomer to the *Z*,*Z* isomer practically vanishes. Comparing the 1:1 binding constants, the difference 5.40 ± 0.45 represents a decrease exceeding five orders of magnitude. We attribute the low binding affinity of the *Z*,*Z* isomer of 2PyDIG to the hypothesized inaccessibility of the two single N–H binding protons of the guanidinium core, which become involved in internal hydrogen bonding to the neighboring pyridine N atoms. Under the same conditions used in the titration of *E*,*E*-2PyDIG with sulfate, no observable change in any chemical shift of *Z*,*Z*-2PyDIG, including the N–H iminoguanidinium protons, could be detected with ^{1}H NMR upon titration of sulfate, while a change in the absorption maximum is observed with absorption spectroscopy. As indicated in the crystal structure (Figure 7), the single N–H groups engage in intramolecular hydrogen bonding to the pyridyl nitrogen atoms. Although no direct interaction of the iminoguanidinium N–H groups of *Z*,*Z*-2PyDIG with sulfate is evident by ^{1}H NMR, *Z*,*Z*-2PyDIG likely does associate partially with sulfate in solution electrostatically. We estimate from the Bjerrum model that the 2PyDIG cation (either isomer) is partially ion-paired under the conditions of the experiments reported herein (Supporting Information). The estimated K_{ass} of 2.95 for 2PyDIG and sulfate implies approximately 36% of the receptor is associated with sulfate. Thus, we interpret the large binding constants for the *E*,*E* isomer to be thermodynamically driven by hydrogen bonding likely assisted by entropy,[30] while the interaction evident by UV-vis spectral changes of the Z,Z isomer upon sulfate addition are taken to be largely electrostatic in origin. The system of reactions involved is diagrammed in Figure 11.

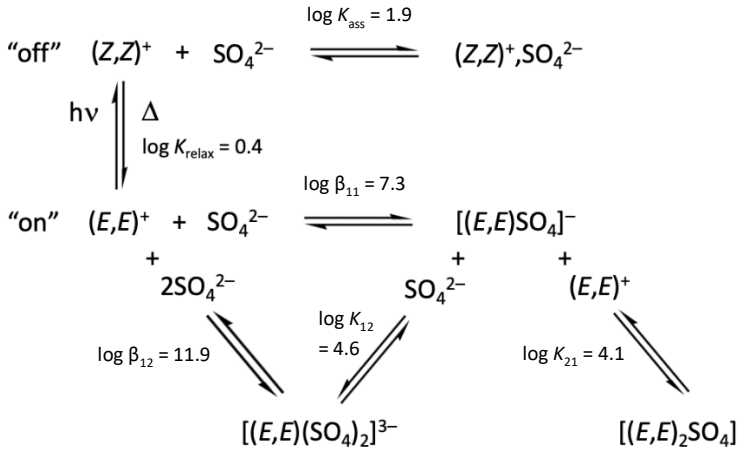

Figure 11. Photoisomerization and associated sulfate-binding equilibria in the 2PyDIG system as characterized in DMSO-d_6.

DFT Calculations

Corroborating calculations on bare 2PyDIG rotamers (Supporting Information, Figure S12) and the interaction of triflate with 2PyDIG were performed at the B3LYP/def2TZVPP level of theory,[34] with higher energy corrections computed using the DLPNO-CCSD(T)/cc-pVTZ theory (see Supporting Information for details).[35] It was observed that the gas-phase complex with the *E*,*E*-isomer remains stable during optimization in the implicit solvent reactive field, but the complex with the *Z*,*Z*-isomer undergoes a structural change, as a hydrogen bond between the NH group and triflate in the gas phase is completely lost in the solvent, showing only a weak hydrogen bond between the much less acidic guanidinium NH_2 group and triflate (Figure 12). A loss of one hydrogen bond from the guanidinium NH group in the Z,Z form is also reflected in the relative free energies of the *E*,*E*- and *Z*,*Z*-forms, with the latter being more stable with no anion (Supporting Information, Figure S12), but less stable in the presence of a weakly coordinating anion (Figure 12). The computed free energy difference between the two forms in the presence of triflate at 25 °C is 1.1 kcal/mol, in good agreement with the experimental value of 0.5 kcal/mol (Eq. 1). This further supports the dramatic decrease in the anion binding affinity upon photoconversion, corroborating the nonbinding behavior of the closed *Z*,*Z* form.

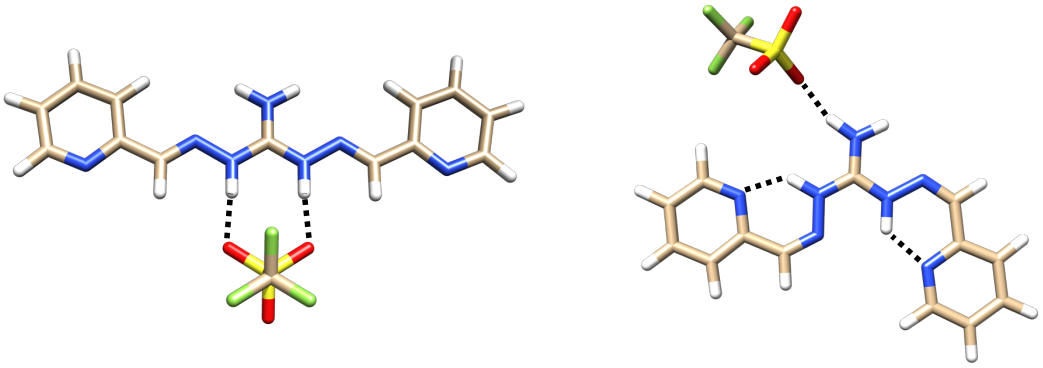

Figure 12. Structures and relative free energies (kcal/mol) of the *E*,*E*- and *Z*,*Z*-forms of 2PyDIG with the triflate anion optimized in the solvent reaction field (DMSO) at the B3LYP/def2TZVPP level[34], with single-point energy corrections using the DLPNO-CCSD(T)/cc-pVTZ theory.[35]

A Photoswitched Sulfate Precipitation-Dissolution Cycle

Excess sulfate precipitates with *E*,*E*-2PyDIG and redissolves with photoirradiation, demonstrating a rudimentary, proof-of-concept binding-release cycle. At higher concentrations in DMSO, the 2PyDIG receptor binds to sulfate as the 1:2 complex (Eq. 4 in Table 1) and precipitates as illustrated in Figure 13. The precipitate instantly forms upon addition of two equivalents of sulfate, putatively assigned as the $[(E,E\text{-2PyDIG})(SO_4)_2]^{2-}$ species. Attempts to obtain crystals suitable for X-ray crystallography have so far proven difficult due to the fast rate of the precipitation; however, addition of 0.5 and 1 equivalents of sulfate does not lead to solid formation, suggesting the solid is the 1:2 complex containing tetramethylammonium counterions. We were able to indirectly determine the amount of precipitated 2PyDIG and relative ratio of PyDIG to sulfate of the precipitate. Upon addition of sulfate to the *E*,*E*-2PyDIG solution, 73.7% of the *E*,*E*-PyDIG

receptor precipitates according to a ^{1}H NMR spectrum of the supernatant. Adding barium chloride to the separated supernatant precipitated the non-interacting sulfate, affording a ratio of sulfate to PyDIG of 2.05. The estimated percentage of sulfate precipitated by gravimetric analysis is 63%. As might be expected, photoirradiating the suspension redissolves the solid, wherein the *E*,*E*-PyDIG undergoes photoisomerization to the *Z,Z* form, ejecting bound sulfate in the process, as summarized in Eq. 6. Over time, the free *Z*,*Z*-PyDIG in solution reverts to the *E*,*E* through a thermal relaxation process, where the $[(E,E\text{-2PyDIG})(SO_4)_2]^{3-}$ species is again precipitated. Making no claim to have made a complete separation that produces a sulfate product with reuse of the co-precipitated receptor, we nevertheless take the results to show that the photoswitching properties of 2PyDIG can be used to effect reversible light-driven phase changes that under practical conditions could potentially be exploited for useful separations.

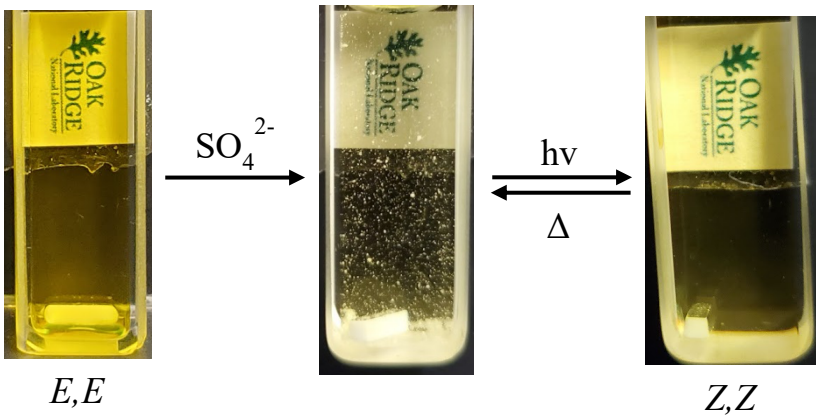

Figure 13. 2PyDIG and sulfate precipitation-redissolution cycling. A solution of 10 mM *E*,*E*-2PyDIG·HOTf in DMSO (left), precipitated $[(E,E\text{-2PyDIG})(SO_4)_2]^{3-}$ upon addition of 2 equivalents of sulfate as tetramethylammonium salt (middle). The precipitate redissolved after UV irradiation (right).

$$[E,E\text{-2PyDIG}]^+ + 2\ SO_4^{2-} \longrightarrow [(E,E\text{-2PyDIG})(SO_4)_2]^{3-}{}_{(s)} \underset{\Delta}{\overset{hv}{\rightleftharpoons}} [Z,Z\text{-2PyDIG}]^+ + 2\ SO_4^{2-} \quad (6)$$

CONCLUSIONS

We have introduced a new photoresponsive chromophore, the diiminoguanidinium group, to stand along with azobenzene, stilbene, acylhydrazone, and similar photoresponsive chromophores as a tool for building photoactivated molecules not only for reversible ion binding, but potentially myriad other chemical functions. The results herein reported confirm our hypothesis of photoswitched binding of sulfate by the 2PyDIG cation, as illustrated in Figure 2. Photoisomerization of the *E*,*E* isomer to the *Z*,*Z* isomer occurs efficiently in DMSO-d_6 induced by UV light, as monitored by ^{1}H NMR and UV-vis absorption spectroscopies. At low concentrations that minimize the apparently bimolecular relaxation process, the photoconversion to the *Z*,*Z* form is nearly quantitative at 95.6 ± 0.4%, exceeding previously reported conversion efficiencies among photoswitchable anion receptors. Intramolecular hydrogen bonding of the guanidinium N–H groups to the pyridines stabilizes the *Z*,*Z* isomer, as evidenced by DFT computations and crystal structures of the binding *E,E* isomer with sulfate and the nonbinding *Z,Z* photoisomer. The exceptional binding of sulfate by the *E*,*E* isomer, involving 1:1, 2:1, and 1:2 receptor:sulfate species, is at least as strong, and likely much stronger, than previously reported monofunctional

guanidinium receptors. Possessing a relatively low pK_a among anion receptors, 2PyDIG exhibits exceptionally strong anion binding via hydrogen bonding that verges on proton transfer. This strong binding of sulfate is diminished by more than five orders of magnitude upon photoisomerization to the *Z,Z* form. Thus, both the *E*,*E*–*Z*,*Z* photoisomerization and the photoswitching of binding and release are exceptionally efficient, and they can be demonstrably exploited for light-driven phase change as shown by the reversible precipitation of the 1:2 complex.

SUPPORTING INFORMATION

Full experimental procedures are provided in the Supporting Information. This includes ligand synthesis, computational methods, photoirradiation studies, X-ray crystallography, titration measurements, ion-pair calculations using the Bjerrum approach, and photoswitched precipitation experiments. CCDC 2092856 and 2092857 contain the supplementary crystallographic data for this paper. These data are provided free of charge by the joint Cambridge Crystallographic Data Centre and Fachinformationszentrum Karlsruhe at http://www.ccdc.cam.ac.uk/structures.

ACKNOWLEDGMENTS

This work was supported by the U.S. Department of Energy, Office of Science, Basic Energy Sciences, Chemical Sciences, Geosciences, and Biosciences Division. This research used resources of the Compute and Data Environment for Science (CADES) at the Oak Ridge National Laboratory and the National Energy Research Scientific Computing Center (NERSC), which are supported by the Office of Science of the U.S. Department of Energy under Contracts No. DE-AC05-00OR22725 and No. DE-AC02-05CH11231, respectively. We would like to acknowledge Drs. Peter Bonnesen, Benjamin Doughty, and Yingzhong Ma for fruitful discussions and advice on experimental design, and Drs. Fabian Bohle and Stefan Grimme at Universität Bonn for providing their code and guidance on the ^{1}H NMR calculations.
The manuscript was produced by UT-Battelle, LLC under Contract No. DE-AC05-00OR22725 with the U.S. Department of Energy. The publisher acknowledges the U.S. Government license to provide public access under the DOE Public Access Plan (http://energy.gov/downloads/doe-public-access-plan).

REFERENCES

[1] a) J.-M. Lehn, Springer Berlin Heidelberg, Berlin, Heidelberg, **1973**, pp. 1-69; b) J.-M. Lehn, in *Supramolecular Chemistry*, **1995**, pp. 11-30.
[2] X. Sun, D. Shabat, S. T. Phillips, E. V. Anslyn, *J. Phys. Org. Chem.* **2018**, *31*, e3827.
[3] a) X. Ji, X. Chi, M. Ahmed, L. Long, J. L. Sessler, *Acc. Chem. Res.* **2019**, *52*, 1915-1927; b) X. Wu, A. M. Gilchrist, P. A. Gale, *Chem* **2020**, *6*, 1296-1309.
[4] B. A. Moyer, J. F. Birdwell, P. V. Bonnesen, L. H. Delmau, in *Macrocyclic Chemistry: Current Trends and Future Perspectives* (Ed.: K. Gloe), Springer Netherlands, Dordrecht, **2005**, pp. 383-405.
[5] S. Shinkai, T. Ogawa, T. Nakaji, Y. Kusano, O. Nanabe, *Tetrahedron Lett.* **1979**, *20*, 4569-4572.

[6] a) S. Shinkai, T. Nakaji, T. Ogawa, K. Shigematsu, O. Manabe, *J. Am. Chem. Soc.* **1981**, *103*, 111-115; b) S. Shinkai, Y. Shirahama, T. Tsubaki, O. Manabe, *J. Am. Chem. Soc.* **1989**, *111*, 5477-5478.
[7] *Anion Coordination Chemistry* (Eds.: K. Bowman-James, A. Bianchi, E. García-España), Wiley-VCH, **2011**.
[8] T. Shimasaki, S.-i. Kato, K. Ideta, K. Goto, T. Shinmyozu, *J. Org. Chem.* **2007**, *72*, 1073-1087.
[9] a) Y. Hua, A. H. Flood, *J. Am. Chem. Soc.* **2010**, *132*, 12838-12840; b) F. C. Parks, Y. Liu, S. Debnath, S. R. Stutsman, K. Raghavachari, A. H. Flood, *J. Am. Chem. Soc.* **2018**, *140*, 17711-17723; c) D. Villarón, M. A. Siegler, S. J. Wezenberg, *Chem, Sci.* **2021**, *12*, 3188-3193; d) S. Xiong, Q. He, *Chem. Commun.* **2021**, *57*, 13514-13517.
[10] Y. Liu, F. C. Parks, E. G. Sheetz, C.-H. Chen, A. H. Flood, *J. Am. Chem. Soc.* **2021**, *143*, 3191-3204.
[11] J.-M. Suk, K.-S. Jeong, *J. Am. Chem. Soc.* **2008**, *130*, 11868-11869.
[12] T. S. C. MacDonald, B. L. Feringa, W. S. Price, S. J. Wezenberg, J. E. Beves, *J. Am. Chem. Soc.* **2020**, *142*, 20014-20020.
[13] Z. Kokan, M. J. Chmielewski, *J. Am. Chem. Soc.* **2018**, *140*, 16010-16014.
[14] a) S. J. Wezenberg, B. L. Feringa, *Org. Lett.* **2017**, *19*, 324-327; b) S. J. Wezenberg, M. Vlatković, J. C. M. Kistemaker, B. L. Feringa, *J. Am. Chem. Soc.* **2014**, *136*, 16784-16787.
[15] S. Lee, A. H. Flood, *J. Phys. Org. Chem.* **2013**, *26*, 79-86.
[16] J. de Jong, B. L. Feringa, S. J. Wezenberg, *ChemPhysChem* **2019**, *20*, 3306-3310.
[17] a) L. Greb, A. Eichhöfer, J.-M. Lehn, *Eur. J. Org. Chem.* **2016**, *2016*, 1243-1246; b) G. Markiewicz, A. Walczak, F. Perlitius, M. Piasecka, J. M. Harrowfield, A. R. Stefankiewicz, *Dalton Trans.* **2018**, *47*, 14254-14262; c) D. J. van Dijken, P. Kovaříček, S. P. Ihrig, S. Hecht, *J. Am. Chem. Soc.* **2015**, *137*, 14982-14991; d) S. M. Landge, E. Tkatchouk, D. Benítez, D. A. Lanfranchi, M. Elhabiri, W. A. Goddard, I. Aprahamian, *J. Am. Chem. Soc.* **2011**, *133*, 9812-9823; e) X. Su, I. Aprahamian, *Chem. Soc. Rev.* **2014**, *43*, 1963-1981.
[18] I. Ravikumar, P. Ghosh, *Chem. Soc. Rev.* **2012**, *41*, 3077-3098.
[19] a) R. Custelcean, N. J. Williams, C. A. Seipp, *Angew. Chem. Int. Ed.* **2015**, *54*, 10525-10529; b) N. J. Williams, C. A. Seipp, K. A. Garrabrant, R. Custelcean, E. Holguin, J. K. Keum, R. J. Ellis, B. A. Moyer, *Chem. Commun.* **2018**, *54*, 10048-10051; c) R. Custelcean, *Chem. Commun.* **2020**, *56*, 10272-10280.
[20] R. J. Abraham, A. J. Stevens, K. A. Young, C. Russell, A. Qvist, M. Khazandi, H. S. Wong, S. Abraham, A. D. Ogunniyi, S. W. Page, R. O'Handley, A. McCluskey, D. J. Trott, *J. Med. Chem.* **2016**, *59*, 2126-2138.
[21] S. Grimme, C. Bannwarth, S. Dohm, A. Hansen, J. Pisarek, P. Pracht, J. Seibert, F. Neese, *Angew. Chem. Int. Ed.* **2017**, *56*, 14763-14769.
[22] G. K. Pierens, T. K. Venkatachalam, D. C. Reutens, *Magn. Reson. Chem.* **2016**, *54*, 298-307.
[23] a) M. Baroncini, S. d'Agostino, G. Bergamini, P. Ceroni, A. Comotti, P. Sozzani, I. Bassanetti, F. Grepioni, T. M. Hernandez, S. Silvi, M. Venturi, A. Credi, *Nat. Chem.* **2015**, *7*, 634-640; b) U. Georgi, P. Reichenbach, U. Oertel, L. M. Eng, B. Voit, *React. Funct. Polym.* **2012**, *72*, 242-251; c) A. Georgiev, A. Stoilova, D. Dimov, D. Yordanov, I. Zhivkov, M. Weiter, *Spectrochim. Acta A Mol. Biomol. Spectrosc.* **2019**, *210*, 230-244; d) J.-L. Schmitt, A.-M. Stadler, N. Kyritsakas, J.-M. Lehn, *Helv. Chim.* **2003**, *86*, 1598-1624.
[24] H. Bouas-Laurent, H. Dürr, *Pure Appl. Chem.* **2001**, *73*, 639-665.

[25] a) S. Ludwanowski, M. Ari, K. Parison, S. Kalthoum, P. Straub, N. Pompe, S. Weber, M. Walter, A. Walther, *Chem. Eur. J.* **2020**, *26*, 13203-13212; b) A. R. E. Carey, S. Eustace, R. A. M. O'Ferrall, B. A. Murray, *J. Chem. Soc., Perkin Trans. 2* **1993**, 2285-2296; c) V. Botti, U. Mazzucato, M. Šindler-Kulyk, A. Spalletti, *J. Photochem. Photobiol. A* **2017**, *333*, 33-39.
[26] C. A. Seipp, N. J. Williams, V. S. Bryantsev, R. Custelcean, B. A. Moyer, *RSC Adv.* **2015**, *5*, 107266-107269.
[27] C. Janiak, *J. Chem. Soc. Dalt. Trans.* **2000**, 3885-3896.
[28] B. Wang, P.-Z. Zhang, X. Chen, A.-Q. Jia, Q.-F. Zhang, *znb* **2018**, *73*, 601.
[29] a) Z. Li, C. Zhang, Y. Ren, J. Yin, S. H. Liu, *Org. Lett.* **2011**, *13*, 6022-6025; b) E. Nord, H. Zhou, S. Rayat, *New J. Chem.* **2021**, *45*, 14184-14192.
[30] M. Berger, F. P. Schmidtchen, *Angew. Chem. Int. Ed.* **1998**, *37*, 2694-2696.
[31] R. Custelcean, K. A. Garrabrant, P. Agullo, N. J. Williams, *Cell. Rep. Phys. Sci.* **2021**, *2*, 100385.
[32] a) K. Kobiro, Y. Inoue, *J. Am. Chem. Soc.* **2003**, *125*, 421-427; b) P. Blondeau, M. Segura, R. Pérez-Fernández, J. de Mendoza, *Chem. Soc. Rev.* **2007**, *36*, 198-210.
[33] a) B. A. Caine, C. Dardonville, P. L. A. Popelier, *ACS Omega* **2018**, *3*, 3835-3850; b) C. Dardonville, B. A. Caine, M. Navarro de la Fuente, G. Martín Herranz, B. Corrales Mariblanca, P. L. A. Popelier, *New J. Chem.* **2017**, *41*, 11016-11028.
[34] a) A. D. Becke, *J. Chem. Phys.* **1993**, *98*, 5648-5652; b) C. Lee, W. Yang, R. G. Parr, *Phys. Rev. B* **1988**, *37*, 785-789.
[35] W. B. Schneider, G. Bistoni, M. Sparta, M. Saitow, C. Riplinger, A. A. Auer, F. Neese, *J. Chem. Theory Comput.* **2016**, *12*, 4778-4792.

Table of Contents

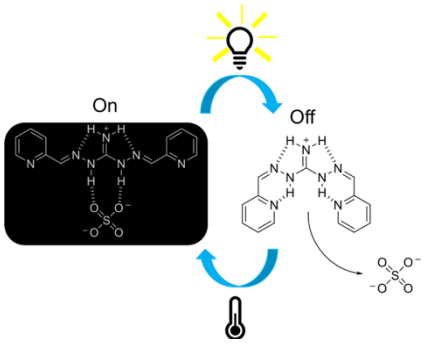

A highly efficient anion receptor with photoswitchable functionality is introduced, based on a new photoresponsive chromophore, the diiminoguanidinium group. *E*,*E*-2-pyridyl-diiminoguanidinium displays more than five orders of magnitude switched-off change in binding strength towards sulfate upon photoirradiation with UV light. The open *E,E* form binds sulfate with extraordinary strength in DMSO, via chelating guanidinium hydrogen bonds. Upon photoisomerization to the *Z,Z* isomer the anion-binding site is shut off by intramolecular hydrogen bonds to the 2-pyridyl substituents, thereby releasing the bound sulfate.